Preparation and performance of noble metal phosphides supported on silica as new hydrodesulfurization catalysts

Preparation and performance of noble metal phosphides supported on silica as new hydrodesulfurization catalysts

Applied Catalysis A: General

Preparation and performance of noble metal phosphides supported on silica as new hydrodesulfurization catalysts

Yasuharu Kanda[a*], Chisato Temma[b], Keisuke Nakata[c], Takao Kobayashi[d], Masatoshi Sugioka[e], and Yoshio Uemichi[a]

[a]Graduate School of Engineering, College of Environmental Technology, Applied Chemistry Research Unit, Muroran Institute of Technology, 27-1 Mizumoto, Muroran 050-8585, Japan

[b]Graduate School of Engineering, Division of Applied Chemistry, Muroran Institute of Technology, 27-1 Mizumoto, Muroran 050-8585, Japan

[c]Graduate School of Engineering, Division of Applied Sciences, Muroran Institute of Technology, 27-1 Mizumoto, Muroran 050-8585, Japan

[d]Technical Division, Muroran Institute of Technology, 27-1 Mizumoto, Muroran 050-8585, Japan

[e]Graduate School of Engineering, College of Design and Manufacturing Technology, Aeronautics and Astronautics Unit, Muroran Institute of Technology, 27-1 Mizumoto, Muroran 050-8585, Japan

* Corresponding author. Tel. and Fax: +81 143 46 5750.

E-mail address: kanda@mmm.muroran-it.ac.jp (Y. Kanda).

Abstract

Preparation of noble metal (NM) (Rh, Pd, Ru, Pt) phosphide species and their catalytic activities for hydrodesulfurization (HDS) of thiophene were investigated. Noble metal phosphides (NM_XP_Y) catalysts were prepared by reduction of P-added NM (NM-P) supported on silica (SiO_2) with hydrogen. Hydrogen consumption peaks at around 350−700 °C, which were attributed to the formation of NM_XP_Y, were observed in temperature-programmed reduction (TPR) spectra of all NM-P/SiO_2. Furthermore, X-ray diffraction (XRD) patterns of NM-P/SiO_2 indicate that NM_XP_Y (Rh_2P, $Pd_{4.8}P$, Ru_2P, PtP_2) were formed by hydrogen reduction at high temperature. The reduction temperature strongly affected HDS activities of NM-P/SiO_2 catalysts. The NM-P/SiO_2 catalysts, other than Pt, showed higher HDS activities than NM/SiO_2 catalysts. The HDS activity of the Rh-P/SiO_2 catalyst was the highest among those of NM-P/SiO_2 catalysts. This activity was higher than that of the Ni-P catalyst and was the same as that of pre-sulfided CoMoP/Al_2O_3 catalyst. Furthermore, the Rh-P/SiO_2 catalyst showed stable activity even after reaction for 30 h. The XRD, transmission electron microscopy (TEM), and energy dispersive X-ray spectroscopy (EDS) results revealed that the formation of small Rh_2P particles and suitable P addition to form Rh_2P caused the high HDS activity of the Rh-P catalyst.

Keywords

Hydrodesulfurization; Thiophene; Noble metal phosphide catalyst

1. Introduction

Recently, the technologies to solve environmental problems, such as acid rain and global warming, have attracted a lot of attention on a global scale. The combustion of organic sulfur compounds in fuels used for boilers and engines results in the formation of sulfur oxides (SO_X), which cause the acid rain. Hydrodesulfurization (HDS) is one of the important processes in the petroleum industry to produce clean fuels [1,2]. $CoMo/Al_2O_3$ catalysts have been widely used in the HDS process. Recently, the petroleum industry claimed that the development of highly active HDS catalysts, which exhibit higher activity than commercial $CoMo/Al_2O_3$ HDS catalysts, will prevent the acid rain and the deactivation of automotive exhaust catalysts [3-6].

Previously, phosphides [7-14], carbides [15-17], and nitrides [15, 18-20] have received much attention as new HDS catalysts. In particular, transition metal phosphides, such as Ni_2P [7-12] and MoP [13, 14], were examined to develop highly active new HDS catalysts. Many preparation methods for metal phosphide catalysts, such as the reduction of oxidized or chlorinated precursors with phosphine (PH_3) and hydrogen, have been reported [20, 21]. Especially, phosphate salts were widely used as phosphorous source. Bussel et al. [10] and Lee and Oyama et al. [11] reported that Ni_2P catalysts supported on silica (SiO_2) showed higher HDS activity than $NiMo/Al_2O_3$ catalysts. Thus, SiO_2 is a superior support for preparation of highly active phosphide catalysts. On the other hand, we have reported that noble metal (NM), especially platinum (Pt), supported on zeolites [22-24] and related materials, such as mesoporous silicates [25-27] and clays [24, 28], showed high and stable activity in HDS of thiophene. Thus, it is expected that noble metal phosphides (NM_XP_Y) show high catalytic activities for HDS reaction, but HDS

activities of NM_XP_Y have not been reported. In the present study, we examined the effect of reduction temperature on the preparation of NM phosphides (NM_xP_y) supported on SiO_2 and their catalytic performance for HDS of thiophene to develop highly active HDS catalysts.

2. Experimental

2.1. Preparation of catalysts

Silica (SiO_2, BET surface area 295 m^2/g) was supplied from Nippon Aerosil Co. NM/SiO_2 catalysts were prepared by an impregnation method using aqueous solutions of NM chlorides such as rhodium (III) chloride trihydrate ($RhCl_3 \cdot 3H_2O$), palladium (II) chloride ($PdCl_2$), ruthenium (III) chloride trihydrate ($RuCl_3 \cdot 3H_2O$), and hydrogen hexachloroplatinate (IV) hexahydrate ($H_2PtCl_6 \cdot 6H_2O$). However, $PdCl_2$ was dissolved in 1.0 mol/l HCl aqueous solution because $PdCl_2$ did not dissolve completely in water. The amount of NM loading was 5 wt.%. Impregnated catalysts were dried at 110 °C for 24 h followed by heat treatment in a nitrogen stream at 450 °C for 1 h to decompose the NM salts. After decomposition of NM salts, catalysts were pressed into disks and crushed to obtain 30–42 mesh size granules. The sieved catalysts were calcined in air at 500 °C for 4 h. The ramp rate of heat treatment and calcination was 10 °C/min. Furthermore, P-added NM(NM-P)/SiO_2 was prepared by the same procedure, using NM chlorides and ammonium dihydrogen phosphate ($NH_4H_2PO_4$) aqueous solution. The amount of P addition was 1.5 wt.%.

2.2. Characterization of catalysts

NM and NM-P supported on SiO_2 were characterized by temperature-programmed reduction (TPR), X-ray diffraction (XRD), and

transmittance electron microscopy (TEM) techniques. TPR spectra were measured using a Shimadzu GC-8A gas chromatograph. Supported NM or NM-P catalysts (0.1 g) were heated in a helium stream (30 ml/min) from room temperature to 500 °C at 10 °C/min, followed by treatment in helium at 500 °C for 1 h. After helium treatment, the calcined catalysts were cooled to 30°C in a helium stream, and the helium was switched into 5 vol% hydrogen-nitrogen (H_2-N_2) mixture gas at 30 °C for 30 min before measurement. Water was removed by a molecular sieve trap. The TPR spectrum was recorded through the temperature range of 30 to 800 °C at 10 °C/min, using a thermal conductivity detector (TCD) to monitor hydrogen consumption. XRD patterns of calcined and reduced catalysts were measured by Rigaku MiniFlex with Cu Kα radiation at 30 kV and 15 mA. Particle (crystallite) size of NM and NM_XP_Y were calculated by Scherrer's equation. TEM observation was carried out using JEOL JEM-2000FX. The conditions of TEM operation were as follows: acceleration voltage = 200 kV and magnification = 200,000. Particle size distribution and average particle size were measured from TEM micrographs. Elemental compositions of NM-P catalysts were determined by semiquantitative analysis using energy dispersive X-ray spectroscopy (EDS, JEOL JED-2300) with Si (Li) semiconductor detector.

2.3. Hydrodesulfurization of thiophene

HDS of thiophene was performed at 350 °C under 0.1 MPa using a conventional fixed bed flow reactor. The 0.1 g amount of catalyst was charged into the quartz reactor and was heated (10 °C/min) in a helium stream (30 ml/min) at 500 °C for 1h. After helium treatment, the catalysts were reduced by hydrogen (30 ml/min) at 350–700 °C for 1 h. The hydrogen-thiophene gas mixture (H_2/Thiophene = 30), obtained by passing a hydrogen stream through a thiophene trap cooled at 0 °C, was

introduced into the reactor. Reaction condition (W/F) was 37.9 g·h/mol. The reaction products were analyzed by gas chromatograph (flame ionization detector, FID) equipped with silicone DC-550 (2 m, 110 °C) and VZ-7 (4 m, 0 °C) columns. Commercial $CoMoP/Al_2O_3$ (Co: 2.5 wt%, Mo: 10.0 wt%, and P: 2.1 wt%) and $Ni\text{-}P/SiO_2$ (prepared using $Ni(NO_3)_3 \cdot 6H_2O$, Ni: 15.0 wt%; P: 7.9%) catalysts were used to compare with supported NM-P catalysts. The pre-sulfided $CoMoP/Al_2O_3$ catalyst was prepared using 5% H_2S-H_2 at 400 °C after hydrogen reduction at 450 °C.

3. Results and discussion

3. 1. TPR spectra of NM-P/SiO_2 catalysts

It is well-known that transition metal phosphides, such as Ni_2P, are prepared by reduction of oxidized precursors at high temperature [8, 10-12]. Therefore, we evaluated the TPR spectra and XRD patterns of $NM\text{-}P/SiO_2$ catalysts to get the information for NM_XP_Y formation by hydrogen reduction. **Figure 1** shows the TPR spectra of calcined NM/SiO_2 catalysts. The hydrogen consumption peaks appeared at 100–200 °C in the spectra of supported Rh and Ru catalysts. These peaks were attributed to reduction of NM oxides. However, there was a remarkable negative peak at 74 °C in the Pd catalyst spectrum. This peak resulted from the decomposition of palladium β hydride [29]. Furthermore, a hydrogen consumption peak did not appear in the low temperature region of the supported Pt catalyst. These results indicate that palladium and platinum oxides are easily reduced into metallic species. No hydrogen consumption peaks appeared in the high temperature region in any TPR spectra of NM/SiO_2 catalysts.

Fig. 2 shows the TPR spectra of $NM\text{-}P/SiO_2$ catalysts. At low temperature

(around 50–200 °C), the peaks were the same as those of NM/SiO_2 catalysts. On the other hand, hydrogen consumption peaks were observed between 200 and 750 °C with all catalysts. In Ru and Pt catalysts, the hydrogen consumption peaks appeared at above 600 °C. Bussel et al. [10] and Lee and Oyama et al. [11, 12] reported that the TPR spectra of supported Ni-P catalysts showed a peak at around 600 °C. These results indicate that the peaks around 600 to 750 °C result from the formation of NM_xP_y. On the other hand, Brock et al. and co-workers [30] reported that reduction of the precursor in a 5% H_2-Ar stream with heating from 50 to 375 °C resulted in the formation of unsupported Rh_2P. We also observed peaks at around 350 °C in the Rh-P and Pd-P catalyst (**Fig. 2 (b)**). These results indicate that Rh and Pd were phosphided at lower temperature than Ru and Pt. The formation of NM_xP_y was identified by XRD patterns of $NM\text{-}P/SiO_2$ catalysts after TPR measurement. **Fig. 3** demonstrates the XRD patterns of $NM\text{-}P/SiO_2$ catalysts after calcination and TPR measurement. The XRD patterns of calcined catalysts revealed that all of the NM catalysts (except Pt) were oxides (Rh_2O_3, PdO, and RuO_2); however, the Pt catalyst was metallic. In contrast, the XRD patterns of Rh-P and Ru-P catalysts after TPR measurement showed clear peaks for NM_xP_y (Rh_2P and Ru_2P). On the other hand, there were small, broad peaks of $Pd_{4.8}P$ in the XRD pattern of Pd-P catalyst. In the Pt-P catalyst, we observed platinum phosphide (PtP_2: 2θ = 27.06°, 31.38°, 44.94°, 53.26°, and 72.30°) and unknown peaks. However, the peaks of metallic Pt (2θ = 39.74°, 46.24°, 67.46°, 81.24°, and 85.70°) were also observed. This result indicates that even if Pt-P was reduced at 800 °C, formation of PtP_2 is insufficient. That is to say, Pt forms phosphide species less easily than other NM. We found that reduction of all $NM\text{-}P/SiO_2$ catalysts with hydrogen resulted in the formation of NM_xP_y species.

3. 2. HDS activities of NM-P/SiO_2 catalysts

Fig. 4 shows the thiophene HDS over NM-P/SiO_2 catalysts reduced at 550 °C. The order of the HDS activities of NM-P/SiO_2 catalysts was Rh-P > Pd-P > Ru-P > Pt-P. Furthermore, we evaluated the reduction temperature on the HDS activities of NM/SiO_2 and NM-P/SiO_2 catalysts. The reduction temperature affected the HDS activities of NM/SiO_2 catalysts minimally, as shown in **Fig. 5 (a)**. On the other hand, the reduction temperature strongly affected the HDS activities of NM-P/SiO_2 catalysts and the type of NM determined the optimal reduction temperature of the NM-P catalysts, as shown in **Fig. 5 (b)**. **Fig. 6** shows the HDS activities of NM-P/SiO_2 and NM/SiO_2 catalysts reduced at optimal temperature. The HDS activities of NM-P/SiO_2 catalysts, except Pt-P catalyst, were higher than those of NM/SiO_2 catalysts. However, the Pt-P/SiO_2 catalyst showed lower activity than the Pt/SiO_2 catalyst. Especially, P addition remarkably enhanced the HDS activity of the Rh/SiO_2 catalyst. Furthermore, this activity was higher than that of the Ni-P catalyst and was the same as the pre-sulfided CoMoP/Al_2O_3 catalyst. The stability of catalytic activity was evaluated by relative activity (A/A_0), which was calculated by the activity at any reaction time (A) divided by the initial activity (A_0, at 10 min). We did not evaluate the A/A_0 of Ru-P and Pt-P catalysts because these catalysts showed remarkably lower activities than other NM-P and CoMoP catalysts. The A/A_0 values of Rh-P/SiO_2, Pd-P/SiO_2 and CoMoP/Al_2O_3 catalysts are listed in **Table 1**. In CoMoP/Al_2O_3 catalyst, the A/A_0 remarkably decreased within the initial 1 h. Then the A/A_0 was stable from 3 h until 30 h. On the other hand, the A/A_0 of Rh-P catalyst slightly decreased with time on stream. Furthermore, this A/A_0 was higher than that of pre-sulfided CoMoP/Al_2O_3 catalyst at any reaction time.

However, the HDS activity of Pd-P/SiO_2 catalyst was remarkably decreased with time on stream. Thus, the Rh-P/SiO_2 catalyst has higher stability and potential for HDS reaction than other NM-P/SiO_2 catalysts. **Table 2** shows the product distribution over NM/SiO_2 and NM-P/SiO_2 catalysts in the HDS of thiophene at 350 °C. The selectivity of n-butane definitely increased with increasing thiophene conversion by P addition. This selectivity for Rh-P catalyst was the same as that for CoMoP/Al_2O_3 catalyst. In contrast, P addition enhanced the thiophene conversion for Pd catalyst, but decreased n-butane selectivity. Furthermore, selectivity of tetrahydrothiophene (THT) for the Pd-P catalyst was remarkably lower than that for other NM-P catalysts. These results mean that the direct desulfurization route preferentially occurred over Pd-P catalyst. We examined the XRD patterns of NM-P/SiO_2 catalysts to clarify activity enhancement by phosphidation of NM.

3. 3. XRD patterns of reduced NM/SiO_2 and NM-P/SiO_2 catalysts

Fig. 7 shows the XRD patterns of NM-P/SiO_2 catalysts with different reduction temperatures. After reduction at 500 °C, we observed a remarkably high intensity of NM_XP_Y (Rh_2P and $Pd_{4.8}P$) in the XRD patterns of Rh and Pd catalysts with high HDS activities. In the XRD patterns of the Ru-P/SiO_2 catalyst reduced at 500 and 550 °C, both Ru and Ru_2P were observed. On the other hand, peaks of platinum phosphides were not observed in the XRD pattern of Pt-P/SiO_2 reduced at 500 and 550 °C. In the TPR spectra of the Ru-P and Pt-P catalysts, hydrogen consumption was observed above 600 °C, as shown in **Fig. 2**. Thus, large peaks of metallic NM species appeared in the XRD patterns of Ru-P and Pt-P catalysts.

The peaks of NM_XP_Y (Rh_2P, $Pd_{4.8}P$, Ru_2P, and PtP_2) species increased with increasing reduction temperature. However, the $Pd_{4.8}P$ peaks decreased and

broadened with increasing reduction temperature. It was reported that $Pd_{4.8}P$ decomposes eutectoidally into Pd_6P and Pd_3P between 660 °C and 700 °C [31]. This indicates that decomposition of $Pd_{4.8}P$ into other palladium phosphides may lead to decrease of $Pd_{4.8}P$ intensity. Therefore, decomposition of $Pd_{4.8}P$ explains the low activities of Pd-P/SiO_2 catalysts reduced at high temperature (above 600 °C, **Fig. 5** (b)).

3. 4. Particle sizes of NM_XP_Y and NM in reduced NM-P/SiO_2 catalysts

Fig. 8 shows the TEM images of NM-P/SiO_2 catalysts reduced at 500 °C. We observed small NM_XP_Y and NM particles in all catalysts. The particle size distributions of NM_XP_Y and NM measured from TEM images of NM-P/SiO_2 catalysts reduced at 500 and 650 °C are shown in **Fig. 9**. Furthermore, **Table 3** shows the average particle size calculated from TEM images and XRD patterns using Scherrer's equation. With the exception of Pt-P, the NM_XP_Y and NM particle size distribution shifted toward larger particle size when reduction temperature increased from 500 to 650 °C, as shown in **Fig. 9**. The particle size distribution of Pt-P/SiO_2 catalyst reduced at 650 °C has two peaks (**Fig. 9**), but the average particle size did not change compared with that of the material reduced at 500 °C (**Table 3**). The particle size of Rh-P/SiO_2 was the smallest among all of the NM-P/SiO_2, as shown in **Table 3**. At both reduction temperatures (500 and 650 °C), the average particle size of Rh-P catalyst measured from TEM was the same as that calculated from XRD. For the Pd-P catalyst reduced at 500 °C, the particle size measured by TEM was also the same as that calculated from XRD. However, for the Pd-P catalyst reduced at 650 °C, the particle size calculated from XRD was remarkably smaller than that calculated from TEM. An explanation of this result is

that particle size calculated from XRD would not be accurate because a broad peak was observed in the XRD pattern (**Fig. 7 (ii), (d)**) due to decomposition of $Pd_{4.8}P$ into other phosphides [31]. On the other hand, the particle sizes of Ru-P and Pt-P catalysts calculated from XRD were larger than those measured from TEM at either reduction temperature. The small amount of large particles may be difficult to observe by TEM. On the other hand, XRD analysis detects large particles as the sharp peaks, as shown in **Fig. 7**. Therefore, TEM observation is not the proper method to estimate average particle diameter of Ru-P and Pt-P catalysts. In contrast, Rh-P and Pd-P catalysts would have uniform particle size because particle size measured from XRD was the same as that from TEM.

3. 5. Elemental analysis by EDS

Table 4 shows the elemental analysis of reduced NM-P/SiO_2 by EDS. The content of NM was 5 wt% in all catalysts, but P content was less than 1.5 wt%. The formation of phosphine explains this result. The measured P/NM molar ratios and stoichiometric P/NM ratios are also listed in **Table 4**. For the Rh-P and Ru-P catalysts, the measured P/NM ratios were slightly higher than the stoichiometric ratio. Wang et al. [8] and Bussel et al. [10] reported that excess P in the catalyst precursor is necessary to prepare highly active Ni-P/SiO_2 catalysts. Thus, the formation of small Rh_2P particles and a suitable P addition to form Rh_2P resulted in the high HDS activity of the Rh-P/SiO_2 catalyst. On the other hand, the measured P/NM ratios of Pd-P catalyst with reduction at 500 and 650 °C were three to five times higher than the stoichiometric ratios. These results indicate that the amount of P added was not suitable to form NM_XP_Y. Therefore, Pd-P catalysts with higher HDS activities than that of the CoMoP/Al_2O_3 catalyst would be prepared by

controlling the amount of P added. The measured P/NM of the Pt-P catalyst was close to the stoichiometric ratio. However, the HDS activity of the Pt-P catalyst was remarkably lower than that of other NM-P and Pt catalysts. An explanation for this result is the poisoning of the active site by P because Pt does not easily form phosphides.

4. Conclusions

NM_XP_Y species were formed on SiO_2 by a conventional preparation method using $NH_4H_2PO_4$. The nature of NM caused variations in the HDS activities of NM-P/SiO_2 catalysts. The order of the activities of these catalysts was as follows: Rh-P > Pd-P > Ru-P > Pt-P. In particular, the HDS activity of the Rh-P catalyst was remarkably higher than that of the Ni-P catalyst and was the same as that of the pre-sulfided CoMoP/Al_2O_3 catalyst. Furthermore, the Rh-P/SiO_2 catalyst showed stable activity even after reaction for 30 h. Characterization of the NM-P catalysts revealed that the formation of small Rh_2P particles and suitable P addition to form Rh_2P caused the high HDS activity of the Rh-P catalyst.

Acknowledgment

This work was supported by a Grant-in-Aid for Young Scientists (B), Japan (21750158). We thank Nippon Aerosil Co. for supplying the silica.

References

[1] H. Topsøe, B.S. Clausen, F.E. Massoth, *Catal.-Sci. Technol.*, 11 (1996) 1-310.

[2] D.D. Whitehurst, T. Isoda, I. Mochida, *Adv. Catal.*, 4 (1998) 345-471.

[3] T. Kabe, A. Ishihara, W. Qian, Hydrodesulfurization and Hydrodenitrogenation Kodansha Scientific, Wiley-VCH, Tokyo, 1999.

[4] C. Song, X. Ma, *Appl. Catal. B: Environ.*, 41 (2003) 207-238.

[5] T. Fujikawa, *J. Jpn. Petrol. Inst.*, 50 (2007) 249-261.

[6] Y. Okamoto, *Catal. Today*, 132 (2009) 9-17.

[7] S. J. Sawhill, D. C. Philips, M. E. Bussell, *J. Catal.*, 215 (2003) 208-219.

[8] A. Wang, L. Ruan Y. Teng, X. Li, M. Lu, J. Rena, Y.Wanga, Y. Hu, *J. Catal.*, 229 (2005) 314-321.

[9] S. Yang, C. Liang, R. Prins, *J. Catal.*, 237 (2006) 118-130.

[10] S. J. Sawhil, K. A. Layman, D. R. Van Wyk, M. H. Engelhard, C. Wang, M. E. Bussell, *J. Catal.*, 231 (2005) 300-313.

[11] Y. K. Lee, S. T. Oyama, *Appl. Catal. A: Gen.*, 322 (2007) 191-204.

[12] S. T. Oyama, Y. K. Lee, *J. Catal.*, 258 (2008) 393-400.

[13] D. C. Phillips, S. J. Sawhill, R. Self, M. E. Bussell, *J. Catal.*, 207 (2002) 266-273.

[14] A. Montesinos-Castellanos, T.A. Zepeda, B. Pawelec, E. Lima, J.L.G. Fierro, A. Olivas, J.A. de los Reyes H., *Appl. Catal. A: Gen.*, 334 (2008) 330-338.

[15] P. A. Aegerter, W.W.C. Quigley, G.J. Simpson, D.D. Ziegler, J.W. Logan, K.R. McCrea, S. Glazier, M. E. Bussell, *J. Catal.*, 164 (1996) 109-121.

[16] B. Dhandapani, T. St. Clair, S.T. Oyama, *Appl. Catal. A*, 168 (1998) 219-228.

[17] M. Lewandowski, A. Szyman´ska-Kolasa, P. Da Costa, C. Sayag, *Catal. Today*, 119 (2007) 31-34.

[18] T. Kadono, T. Kubota, Y. Okamoto, *Catal. Today*, 87 (2003) 107-115.

[19] M. Nagai, *Appl. Catal. A: Gen.*, 322 (2007) 178-190.

[20] S. T. Oyama, *J. Catal.*, 216 (2003) 343-352.

[21] S. T. Oyama, T. Gott, H. Zhao, Y.K. Lee, *Catal. Today*, 143 (2009) 94-107.

[22] M. Sugioka, F. Sado, Y. Matsumoto, N. Maesaki, *Catal. Today*, 29 (1996) 255-259.

[23] M. Sugioka, F. Sado, T. Kurosaka, X. Wang, *Catal. Today*, 45 (1998) 327-334.

[24] M. Sugioka, T. Kurosaka, *J. Jpn. Petrol. Inst.*, 45 (2002) 342-354.

[25] Y. Kanda, T. Kobayashi, Y. Uemichi, S. Namba, M. Sugioka, *Appl. Catal. A: Gen.*, 308 (2006) 111-118.

[26] Y. Kanda, T. Aizawa, Y. Uemichi, M. Sugioka, S. Namba, *Appl. Catal. B: Environ.*, 77 (2007) 117-124.

[27] Y. Kanda, A. Seino, T. Kobayashi, Y. Uemichi, M. Sugioka, *J. Jpn. Petrol. Inst.*, 52 (2009) 42-50.

[28] Y. Kanda, H. Iwamoto, T. Kobayashi, Y. Uemichi, M. Sugioka, *Top. Catal.*, 52 (2009) 765-771.

[29] G. Lieltza, M. Nimza, J. Völtera, K. Läzärb, L. Guczib *Appl. Catal.*, 45 (1988) 71-83.

[30] C. M. Sweeney, K. L. Stamm, S. L. Brock, *J. Alloys Compd.*, 448 (2008) 122-127.

[31] L.O. Gullman, *J. Less-Comm. Metals*, 11 (1966) 157-167.

Table 1

Relative activities of NM-P/SiO_2 catalysts for HDS of thiophene at 350 °C

Catalyst	Reduction Temperature (°C)	Relative activity (A/A_0)			
		1 h	3 h	15 h	30 h
Rh-P	550	0.979	0.970	0.920	0.889
Pd-P	500	0.900	0.860	0.728	0.677
CoMoP/Al_2O_3	400 (sulfidation)	0.884	0.851	0.843	0.830

A_0: Activity at 10 min

A: Activity at any reaction time

Table 2

Distribution of reaction products in the HDS of thiophene over reduced NM/SiO_2 and $NM\text{-}P/SiO_2$ catalysts

Catalyst	Reduction temperature (°C)	Conversion (%)	Composition of HDS products (%)				
			C_1-C_3[a)]	Butanes	Butenes	1,3-butadiene	THT[b)]
Rh	450	13.32	0.00	12.13	85.28	0.00	2.59
Rh-P	550	54.95	0.11	20.82	75.54	0.00	3.53
Pd	350	39.86	0.00	26.96	70.38	0.00	2.66
Pd-P	500	45.85	1.06	10.04	87.48	0.00	1.42
Ru	350	0.28	0.00	0.00	77.81	22.19	0.00
Ru-P	650	12.66	0.00	4.94	86.85	0.00	8.21
Pt	400	22.09	0.00	52.05	41.48	0.00	6.47
Pt-P	650	3.36	0.00	14.25	60.15	0.00	25.60
CoMoP $/Al_2O_3$	400 (Sulfidation)	53.28	0.70	18.68	80.53	0.00	0.10

a) C_1-C_3 hydrocarbons

b) Tetrahydrothiophene

Table 3

Particle size of noble metal phosphides in NM-P/SiO_2 catalysts calculated by TEM images and XRD patterns using Scherrer's equation

Catalyst	Reduction temperature (°C)	Average particle size (nm)	
		TEM	XRD NM_XP_Y / NM
Rh-P	500	8.3	9.1 / -
	650	9.9	10.8 / -
Pd-P	500	10.2	11.4 / -
	650	13.1	6.0 / -
Ru-P	500	10.0	17.9 / 7.5
	650	11.9	21.7 / -
Pt-P	500	14.9	- / 36.5
	650	14.9	57.5 / 24.4

Table 4

Elemental composition of reduced NM-P/SiO_2 catalysts

Catalyst	Reduction temperature (°C)	Elemental composition measured by EDS			Stoichiometric P/NM of NM_XP_Y observed by XRD
		NM (wt%)	P (wt%)	P/NM (mol/mol)	
Rh-P	500	5.00	1.04	0.69	0.50 (Rh_2P)
	650	5.01	0.99	0.65	0.50 (Rh_2P)
Pd-P	500	5.06	1.43	0.97	0.21 ($Pd_{4.8}P$)
	650	4.99	1.01	0.70	0.21 ($Pd_{4.8}P$)
Ru-P	500	4.99	1.20	0.80	0.50 (Ru_2P)
	650	5.02	0.95	0.63	0.50 (Ru_2P)
Pt-P	500	4.96	1.43	1.82	-
	650	5.04	1.17	1.46	2.00 (PtP_2)

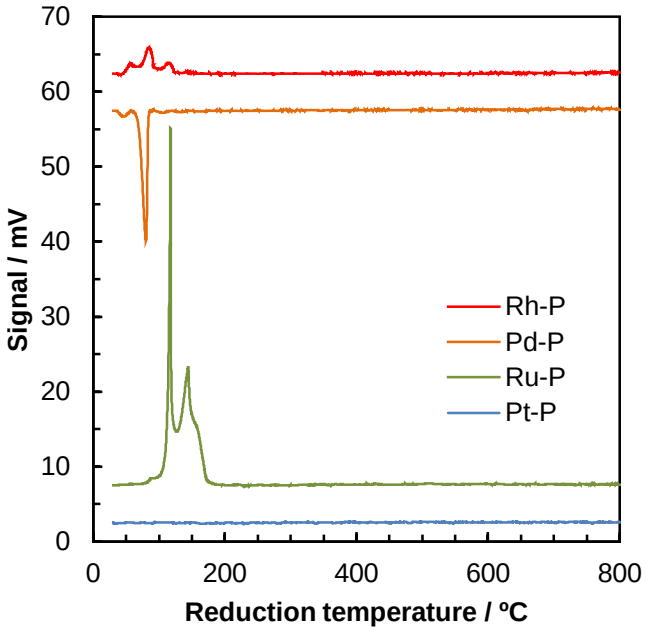

Fig. 1 TPR spectra of calcined NM/SiO_2 catalysts.

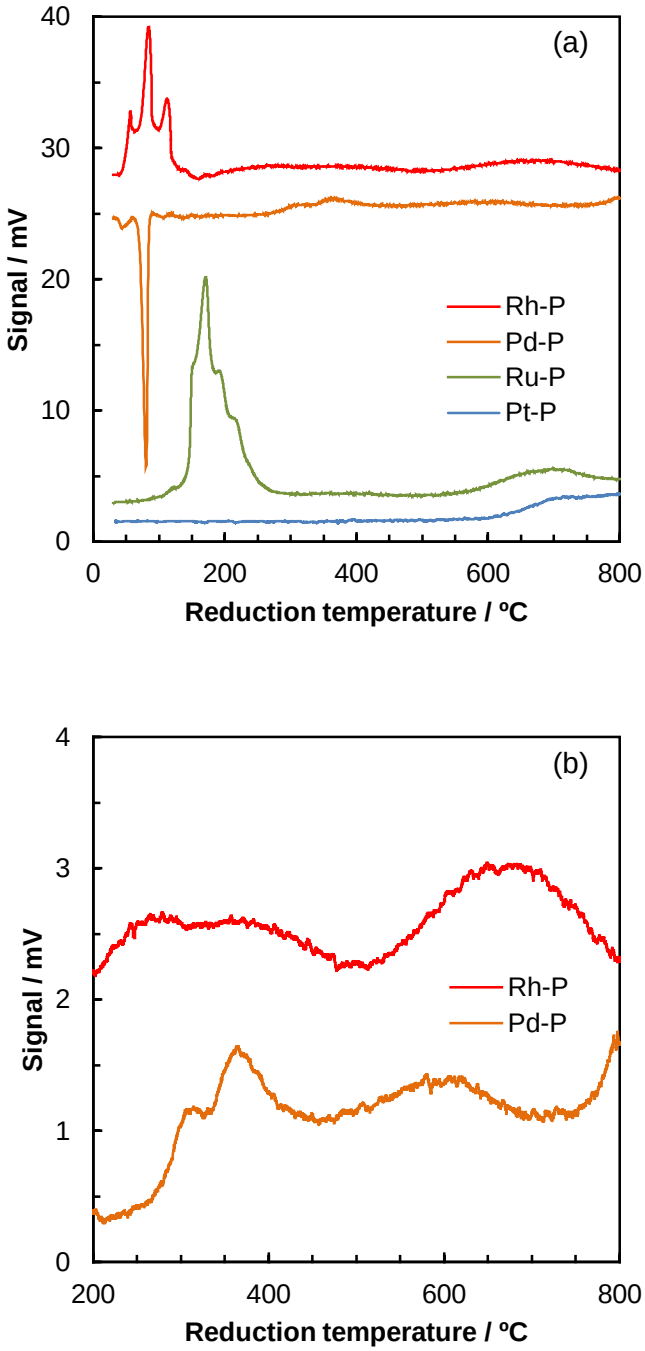

Fig. 2 TPR spectra of calcined NM-P/SiO_2 catalysts. (a) TPR spectra of NM-P catalysts, (b) Magnified TPR spectra of Rh-P and Pd-P catalysts from 200 to 800 °C.

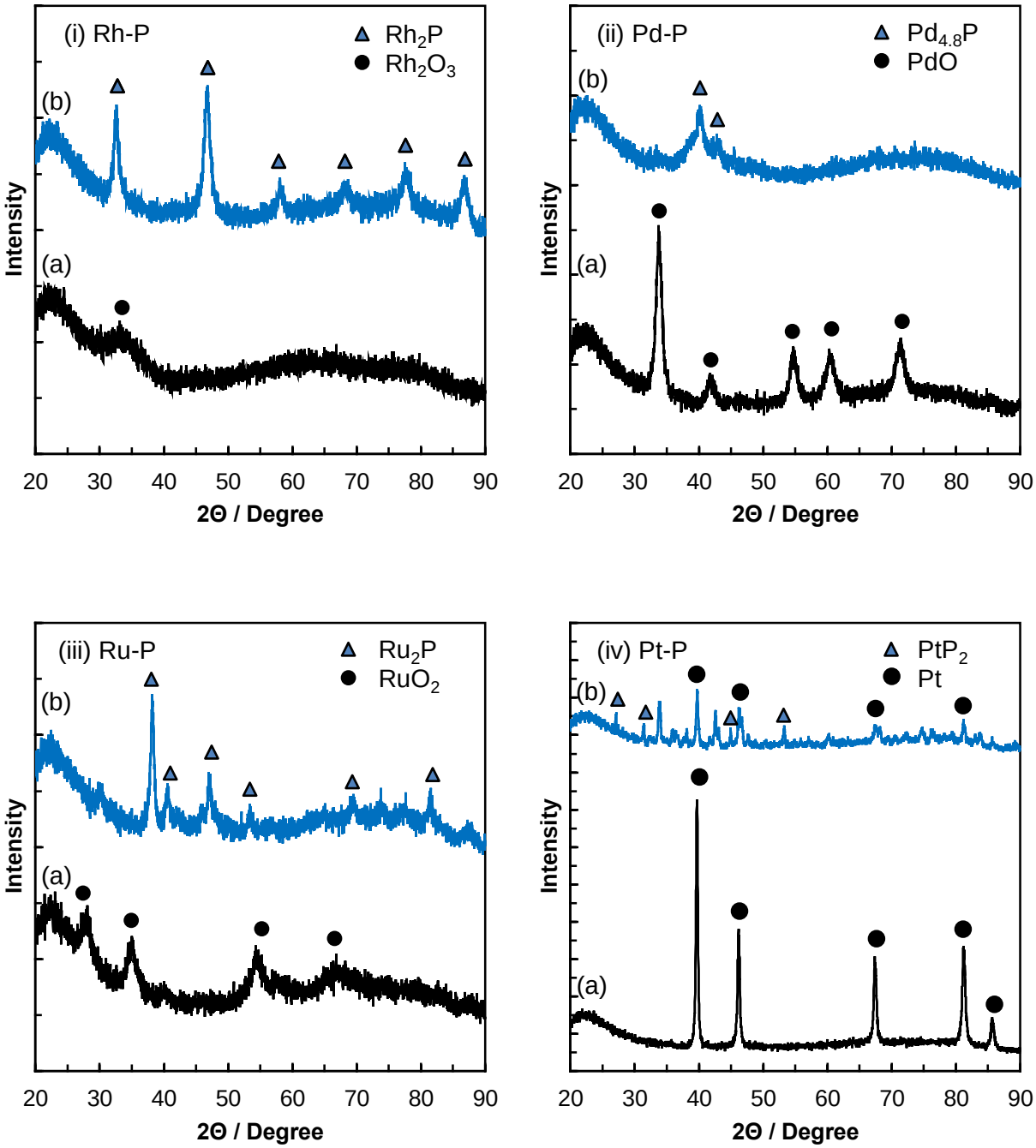

Fig. 3 XRD patterns of NM-P/SiO_2 catalysts after (a) calcination at 500 °C and (b) TPR measurement. (i) Rh-P, (ii) Pd-P, (iii) Ru-P, and (iv) Pt-P.

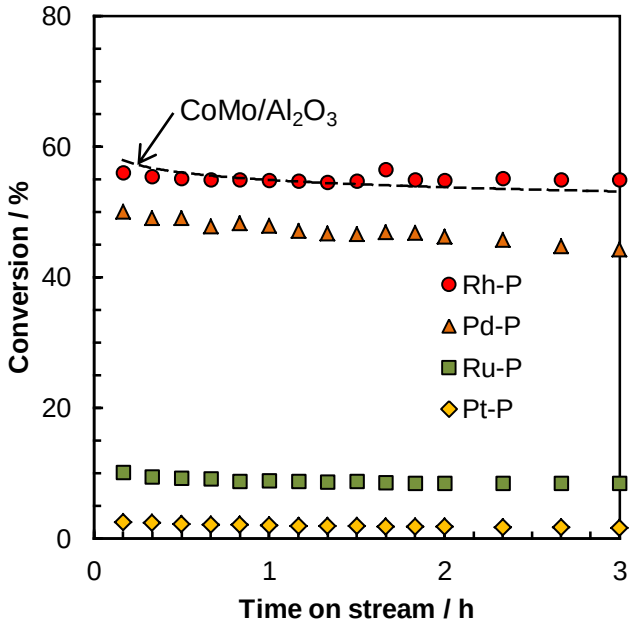

Fig. 4 Hydrodesulfurization of thiophene over NM-P/SiO_2 catalysts reduced at 550 °C.

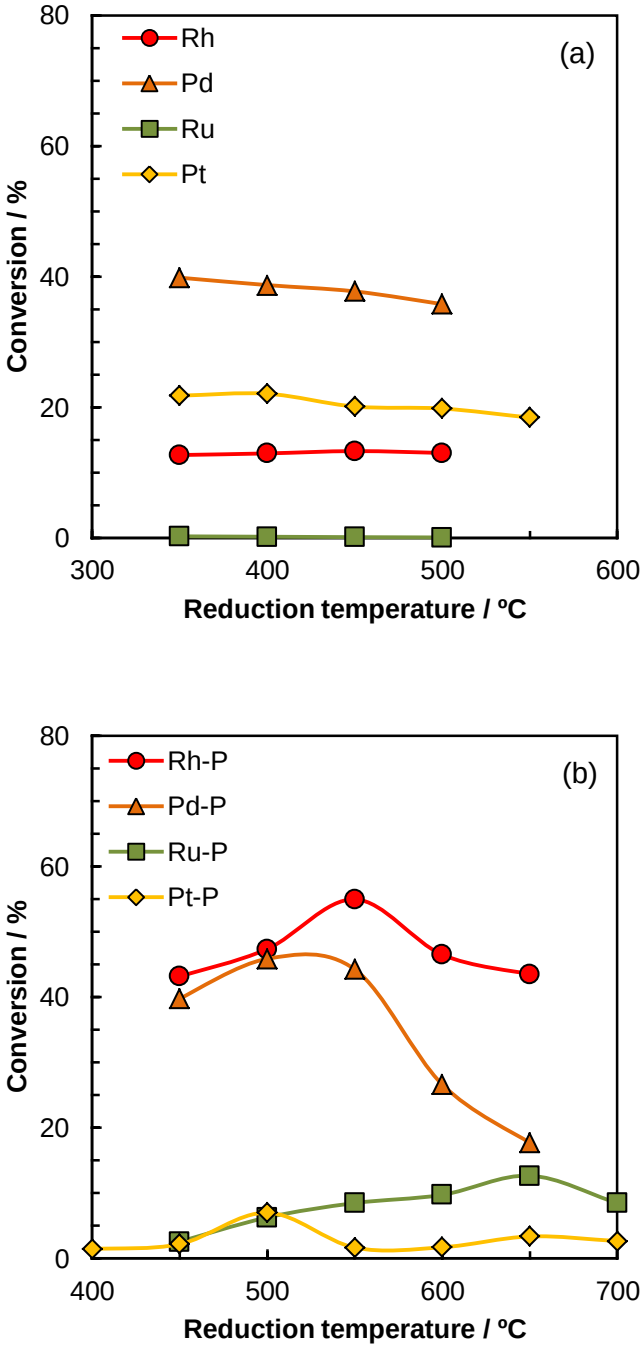

Fig. 5 Effect of reduction temperature on HDS activities of (a) NM/SiO_2 and (b) NM-P/SiO_2 catalysts.

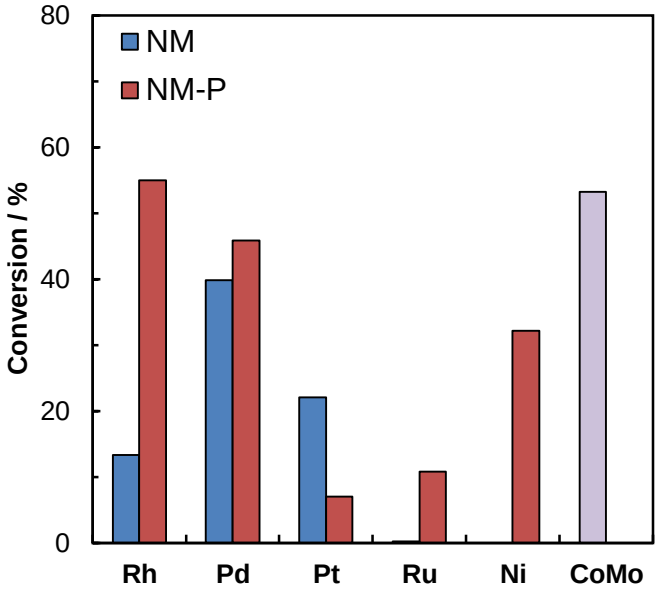

Fig. 6 HDS activities of NM/SiO_2 and NM-P/SiO_2 catalysts. Reduction temperature: 350 °C (Pd), 400 °C (Pt, Ru), 450 °C (Rh), 500 °C (Pd-P, Pt-P), 550 °C (Rh-P), 650 °C (Ru-P, Ni-P).

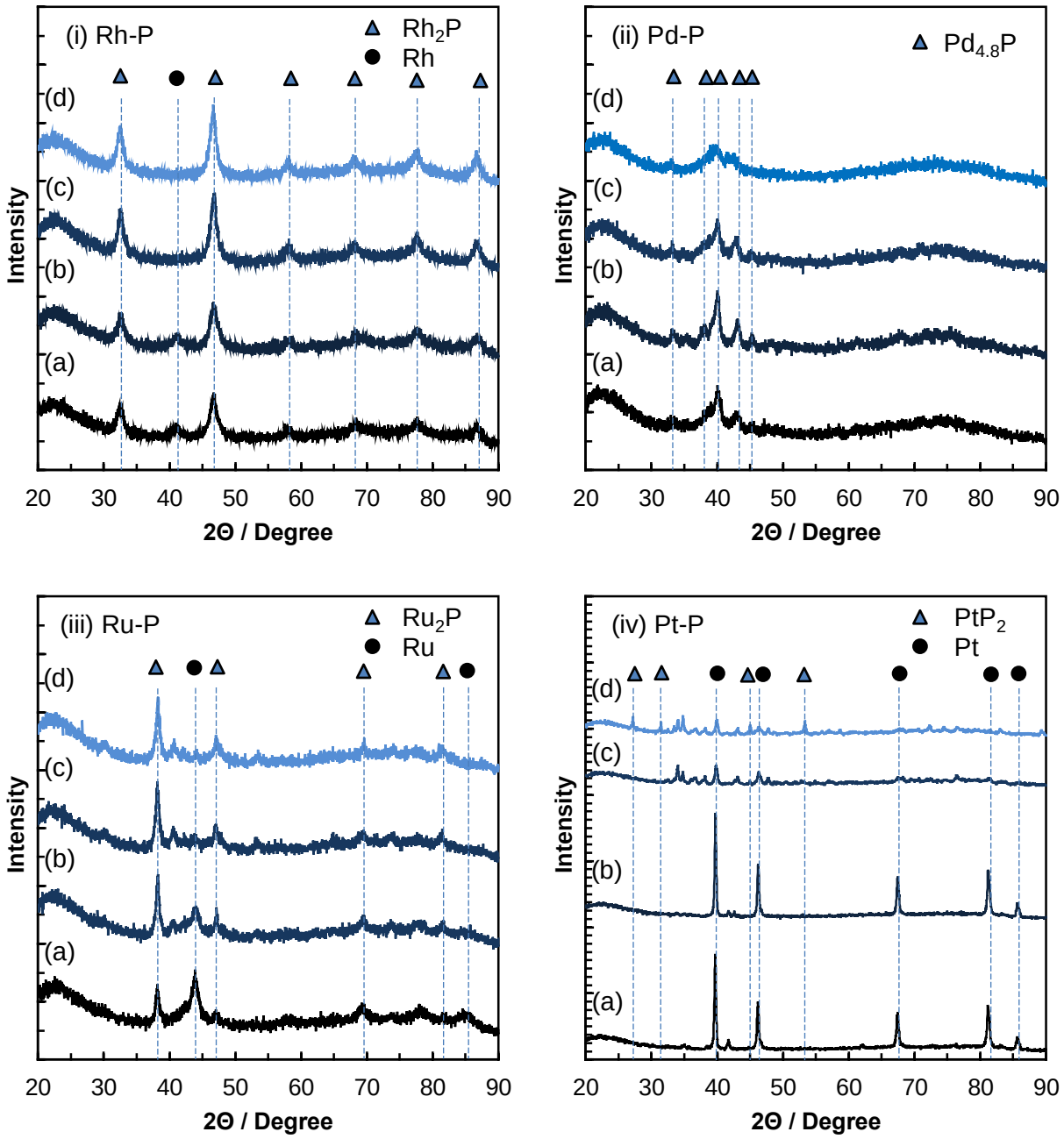

Fig. 7 XRD patterns of NM-P/SiO_2 catalysts after reduction at (a) 500 °C, (b) 550 °C, (c) 600 °C, and (d) 650 °C. (i) Rh-P, (ii) Pd-P, (iii) Ru-P, and (iv) Pt-P.

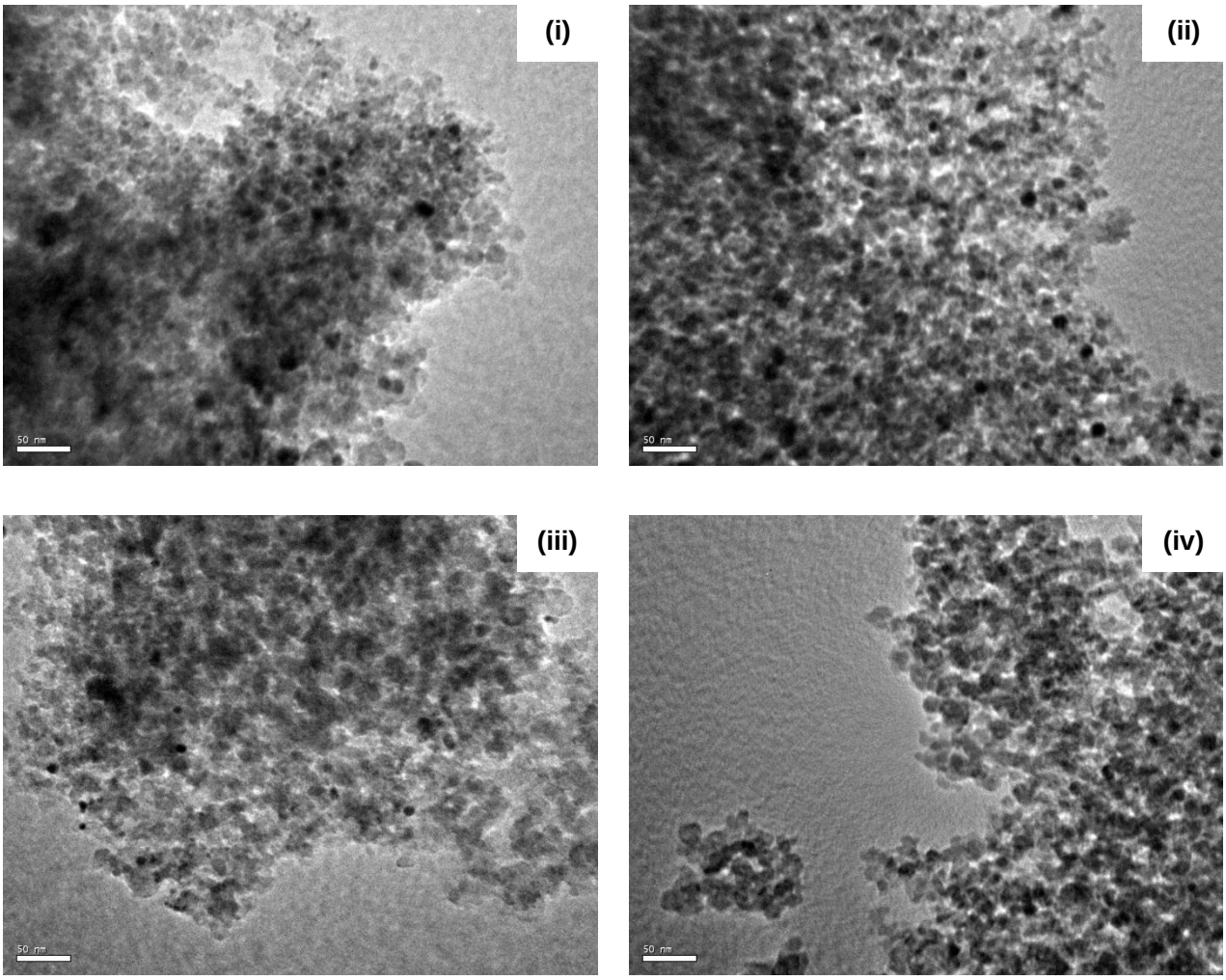

Fig. 8 TEM images of NM-P/SiO_2 catalysts reduced at 500 °C. (i) Rh-P, (ii) Pd-P, (iii) Ru-P, and (iv) Pt-P.

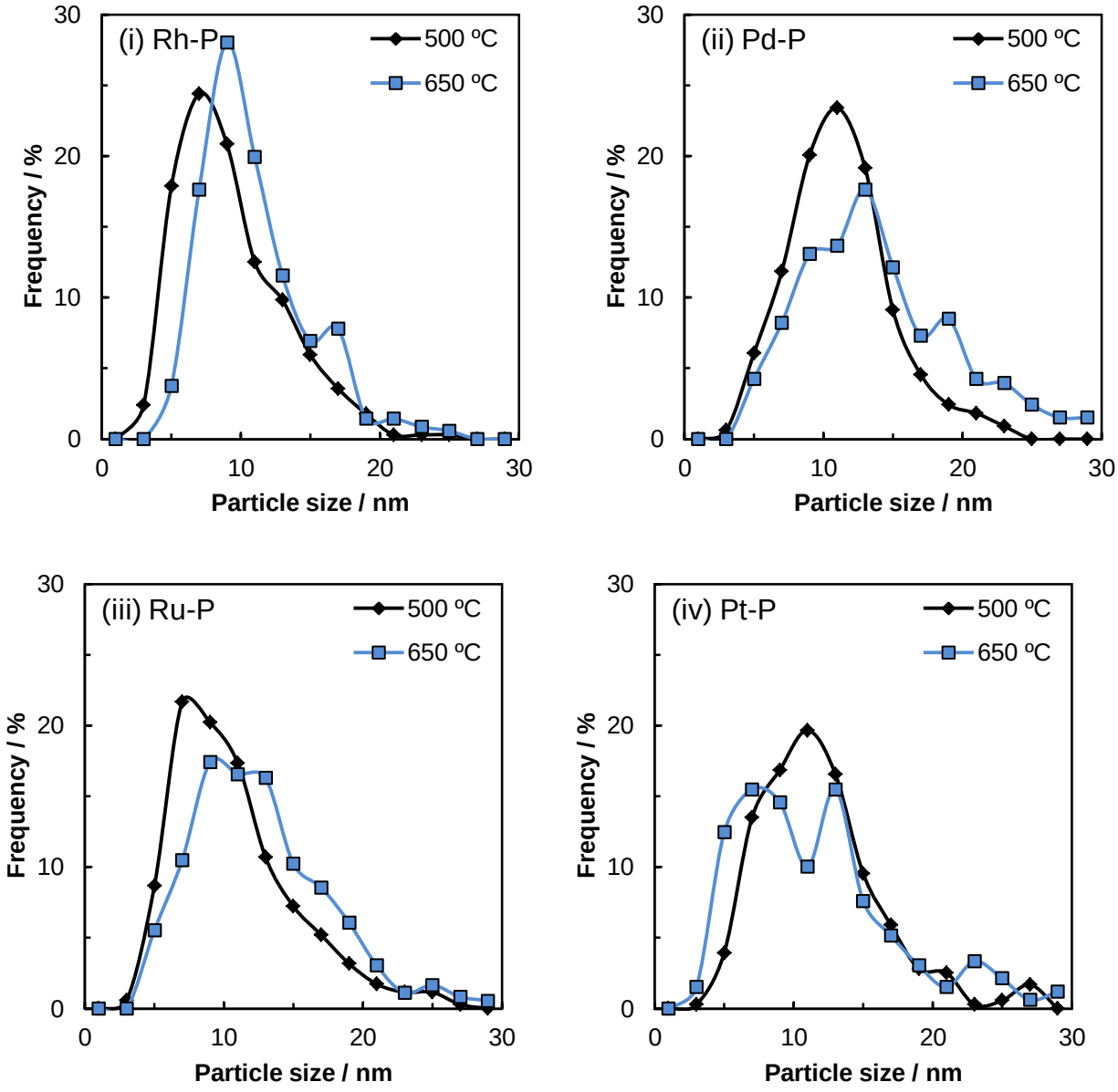

Fig. 9 Particle size distributions of NM and NM_XP_Y in NM-P/SiO_2 catalysts reduced at 500 and 650 °C. (i) Rh-P, (ii) Pd-P, (iii) Ru-P, and (iv) Pt-P.